Redox Biology 50 (2022) 102260

Contents lists available at ScienceDirect

Redox Biology

journal homepage: www.elsevier.com/locate/redox

Upregulation of TIPE1 in tubular epithelial cell aggravates diabetic nephropathy by disrupting PHB2 mediated mitophagy

Lei Liu [a,b], Fang Bai [b], Hui Song [a], Rong Xiao [a], Yuzhen Wang [a], Huimin Yang [b], Xiaolei Ren [a], Shuangjie Li [a], Lifen Gao [a,c], Chunhong Ma [a,c], Xiangdong Yang [b,**], Xiaohong Liang [a,c,*]

[a] Key Laboratory for Experimental Teratology of Ministry of Education and Department of Immunology, School of Basic Medical Sciences, Cheeloo Medical College, Shandong University, Jinan, Shandong, China
[b] Department of Nephropathy, Qilu Hospital of Shandong University, Cheeloo Medical College, Shandong University, Jinan, Shandong, Jinan, Shandong, PR China
[c] Shandong Collaborative Innovation Center of Technology and Equipment for Biological Diagnosis and Therapy, Jinan, Shandong, China

ARTICLE INFO

Keywords:
Diabetic nephropathy
Renal tubular epithelial cells
TIPE1
Mitophagy
PHB2

ABSTRACT

Renal tubular epithelial cells (RTECs) are one of the most mitochondria-rich cell types, and are thus vulnerable to mitochondrial dysregulation, which is defined as a pivotal event in tubular damage in diabetic nephropathy (DN). However, the underlying mechanisms remain largely unknown. Here, we investigated the role and mechanisms of tumor necrosis factor alpha-induced protein 8-like 1 (TNFAIP8L1/TIPE1) in high glucose (HG)-induced mitochondrial dysfunction in RTECs and DN progression. TIPE1 expression was predominantly upregulated in RTECs in patients with DN and mice with streptozotocin (STZ)-induced DN. Conditional knockout of *Tipe1* in RTECs significantly decreased the urine protein creatinine ratio, renal tubular damage, epithelial-mesenchymal transition, and interstitial fibrosis in STZ-induced mice. RNA sequencing revealed that citrate cycle-related genes were positively enriched in the renal tissues of RTEC-specific *Tipe1* knockout mice. *Tipe1* deficiency upregulated ATP levels, mitochondrial membrane potential, and respiration rate, but downregulated mitochondrial ROS levels in RTECs. Furthermore, *Tipe1* ablation led to enhanced mitophagy in RTECs, indicative of increased LC3II, PINK1, and Parkin expression, but decreased p62 expression in mitochondria. Mechanistically, mass spectrometry screening and co-immunoprecipitation assays revealed the interaction of TIPE1 with prohibitin 2 (PHB2), a crucial mitophagy receptor. Intriguingly, TIPE1 promoted the ubiquitination and proteasomal degradation of PHB2. Subsequently, PHB2 knockdown almost abrogated the improvement of *Tipe1* loss on HG-induced tubular cell mitophagy and damage. Thus, TIPE1 disrupts mitochondrial homeostasis in RTECs and promotes tubular damage by destabilizing PHB2 under HG conditions. Hence, TIPE1 may act as a potential therapeutic target to prevent DN progression.

1. Introduction

Diabetic nephropathy (DN) is one of the most devastating complications of diabetes and the major global cause of end-stage renal disease [1], which is characterized by proteinuria, mesangial matrix overproduction, renal hypertrophy, and fibrosis. Several factors, including the accumulation of advanced glycation end-products (AGEs), activation of protein kinase C (PKC), renin-angiotensin system (RAS), TGF-β signaling pathway, and oxidative stress, have been shown to be involved in the pathogenesis of DN [2,3]. However, over the last several decades, only a few drugs such as RAS and SGLT2 inhibitors were used to prevent the progression of DN or to improve renal function [4,5]. Until now, DN accounts for up to 20%–40% of individuals who require renal replacement therapy worldwide, leading to more than 950,000 deaths globally every year [6,7]. Thus, unravelling the novel molecular pathways involved in the progression of DN would address the urgent need to identify potential therapeutic targets to slow down or even reverse kidney dysfunction.

Abbreviations: RTEC, Renal tubular epithelial cell; DN, diabetic nephropathy; TNFAIP8L1/TIPE1, tumor necrosis factor alpha-induced protein 8-like 1.

* Corresponding author. Key Laboratory for Experimental Teratology of Ministry of Education and Department of Immunology; School of Basic Medical Sciences, Cheeloo Medical College, Shandong University, Jinan, 250012, China.
** Corresponding author. Department of Nephropathy, Qilu Hospital of Shandong University; Cheeloo Medical College, Shandong University, Jinan, 250000, China.
E-mail address: liangxiaohong@email.sdu.edu.cn (X. Liang).

https://doi.org/10.1016/j.redox.2022.102260
Received 5 January 2022; Received in revised form 1 February 2022; Accepted 4 February 2022
Available online 7 February 2022

Emerging evidence has demonstrated that tubular injury and tubulointerstitial fibrosis largely contribute to and are closely correlated with renal malfunction, which further predicts the prognosis of DN [8,9]. Upon persistent exposure to high-glucose (HG) ambiance, hemodynamics, oxidative stress, and inflammation, renal tubular epithelial cells (RTECs) are induced to undergo cell death, senescence and epithelial-mesenchymal transition (EMT), which in turn leads to interstitial inflammation and fibrosis [10]. Notably, tubular cell death is a major feature of experimental and human DN that leads to renal cell loss and tubular atrophy [11,12]. Multiple crucial regulatory molecules and signaling pathways have been reported to mediate tubular cell apoptosis [13]. Importantly, as one of the most mitochondria-rich cell types, RTECs are vulnerable to mitochondrial dysfunction, which is demonstrated to be a pivotal event to mediate their death [14–18]. Furthermore, subsequent features of DN (e.g. albuminuria and renal inflammation) are additional triggers of cell death and may continuously drive disease progression even after adequate control of blood glucose levels, providing a strong rationale for the application of strategies against RTEC cell death in DN.

The tumor necrosis factor-alpha (TNF-α)-induced protein 8 family consists of four members, TIPE (TNFAIP8), TIPE1 (TNFAIP8L1), TIPE2 (TNFAIP8L2), and TIPE3 (TNFAIP8L3). These proteins share a high degree of homology in amino acid sequence and protein structure, and have a unique death effector domain (DED), but play distinct roles in regulating cell death and inflammation [19]. The roles of the TIPE family in DN remain largely unknown. Zhang et al. [20] reported that both TIPE and TIPE2 were markedly increased in the glomeruli of diabetic rats and patients, suggesting that they may play pivotal roles in the development of glomerulosclerosis in DN. TIPE1 is a recently identified TIPE family member that was first identified as a candidate player in both necroptosis and apoptosis [21]. Later, TIPE1 was reported to have diverging roles, either in promoting or suppressing tumor development via modulating the apoptosis or autophagy of different types of tumor cells [22,23]. Notably, TIPE1 was found to regulate Caspase 9, an initiator of the mitochondrial apoptosis pathway, in lung cancer cells and to thereby inhibit tumor growth [24]. Together, these studies suggested that TIPE1 might play versatile roles in regulating cell death and dictating cell fate. Interestingly, immunohistochemical staining revealed the enriched expression of TIPE1 both in proximal convoluted tubules and distal convoluted tubules [25]. However, the role of TIPE1 in DN has not been explored yet.

In the present study, we found that TIPE1 expression was predominantly upregulated in the tubular cells of diabetic patients and mice. Conditional knockout of *Tipe1* in RTECs significantly alleviates renal functional damage, tubular epithelial cell apoptosis, and interstitial fibrosis. Mechanistically, TIPE1 impairs the mitophagy of tubular cells by interacting with and promoting the proteasomal degradation of PHB2, which in turn leads to mitochondrial dysfunction and tubular cell damage. Hence, TIPE1 may be considered as a therapeutic target to prevent DN progression.

2. Materials and methods

2.1. Human kidney tissue samples

Human kidney biopsy samples from patients with diabetic nephropathy and minor lesions were obtained from the Department of Pathology, Qilu Hospital, affiliated with Shandong University. This study was approved by the Research Ethics Committee of Shandong University, and informed consent was obtained from all patients. All information about the human subjects is summarized in Online Table S1.

2.2. Mice and animal models

Eight-week-old male C57BL/6 mice were purchased from the Xinjian Biotechnology Company (Jinan, China). RTEC-specific *Tipe1* deficient mice (T1KO) were generated by crossing Tipe1$^{flox/flox}$ mice with Ksp-Cre mice, which express Cre recombinase in epithelial cells of the renal tubules (Kindly provided by Professor Yi Fan, School of Basic Medicine, Shandong University). To induce DN, wild-type (WT) or T1KO mice were intraperitoneally injected with STZ (80 mg/kg) daily for 3 days after the removal of one kidney. All mice were housed with unrestricted access to food and water, in accordance with the procedures of the Institutional Animal Care and Use Committee of Shandong University.

2.3. Cell cultures and treatment

The human proximal tubular cell line HK-2 was purchased from the National Collection of Authenticated Cell Cultures and cultured in Dulbecco's modified Eagle's medium (c11885500BT, Gibco) supplemented with 10% fetal bovine serum (10270-106, Gibco) and 1% penicillin-streptomycin (p1400, Solarbio) at 37 °C in a humidified atmosphere of 5% CO_2. For HG treatment, HK-2 cells were exposed to complete culture medium supplemented with 25 mM and 40 mM D-glucose for 48 h [26,27]. Cells cultured with 5.5 mM D-glucose or 40 mM mannitol were used as controls.

To knock down TIPE1 and PHB2 expression, HK-2 cells were stably infected with lentivirus containing the corresponding short hairpin RNAs (Lv-shTIPE1 or Lv-PHB2) or negative control lentivirus (Lv-NC) (Table S2). To inhibit mitophagy, HK-2 cells were pretreated with 5 μM Mdivi-1 for 6 h before exposure to different concentrations of D-glucose.

2.4. RNA sequencing analysis

WT and T1KO mice were injected with STZ-induced DN. After 8 weeks, total RNA was extracted from the renal cortical tissues of WT and T1KO mice. RNA sequencing was performed by the Beijing Genomics Institute (BGI) following standard protocols. Libraries were sequenced using the BGISEQ-500 platform.

2.5. Transmission electron microscopy (TEM)

Renal cortical tissues from WT or T1KO mice with DN were subjected to TEM analysis. Briefly, the renal tissues were sliced into 1 mm^3 pieces and immersed in 2.5% glutaraldehyde. Kidney tissues were rinsed with 0.1 M phosphoric acid and fixed with osmic acid for 30 min. Sections were then dehydrated and embedded in acetone. 50–60 nm sections were stained with 3% uranium acetate-lead sodium citrate. Images were captured by Jindi Medical Technology, Jinan, Shandong Province.

2.6. Co-immunoprecipitation

Cell lysates were incubated with anti-PHB2 or anti-HA antibodies and rotated overnight at 4 °C, followed by incubation with protein A/G magnetic beads for 4 h. Subsequently, the complex was pelleted and washed with PBST buffer five times. The pellet was suspended in 1 × SDS sample buffer, boiled, and subjected to SDS-PAGE for Western blot analysis.

2.7. Detection of mitochondrial mass, membrane potential, and ROS level

Mitochondrial ROS in HK-2 cells were measured using a mitochondrial superoxide indicator, following the manufacturer's instructions. Briefly, cells were washed twice with PBS to remove the medium and subsequently incubated in 5 μM MitoSOX Red at 37 °C for 10 min, followed by washing with PBS three times. Cells were then detected by flow cytometry. To measure mitochondrial membrane potential, cells were incubated with MitoTracker Deep Red FM, analyzed by flow cytometry on Cytoflex S (Beckman) or Gallios (Beckman), and analyzed by FlowJo. ROS levels in renal tissue were estimated using DHE staining (sc0063, Beyotime). Briefly, frozen kidney sections were steeped in acetone for 30 min and incubated with DHE (5 μM) for 30 min at 37 °C. Images were

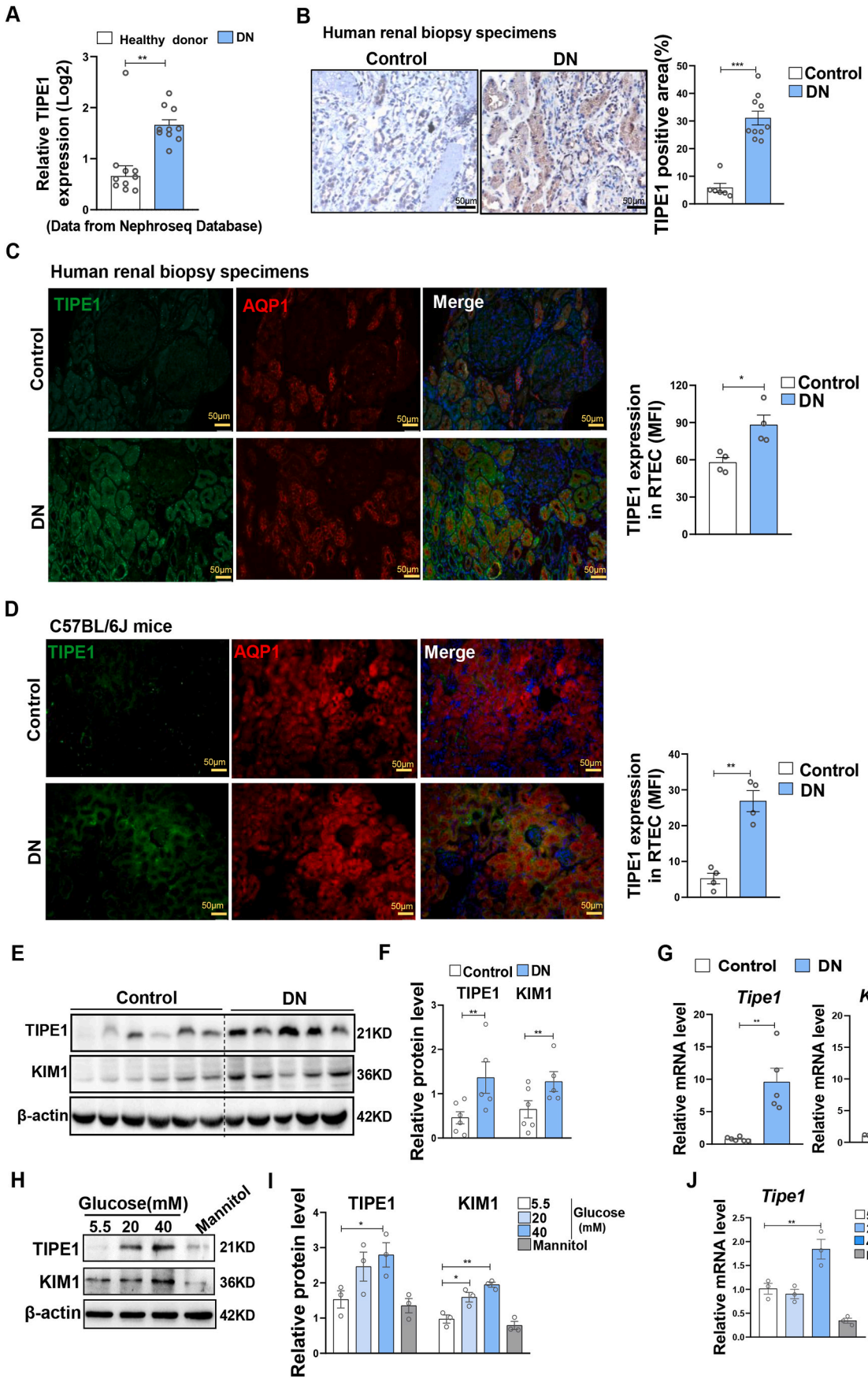

(caption on next page)

Fig. 1. TIPE1 is significantly upregulated in RTECs from DN patients and mice.
A: Analysis of TIPE1 expression in the kidney tissues of DN patients using data from the Nephroseq Database. **B**: Representative images and statistical graphs of immunohistochemical staining for TIPE1 in renal cortical tissue from patients with DN (n = 10) and patients with minor lesions (n = 6). Bar = 50 μm. **C**: Representative images and statistical graphs of immunofluorescent staining for TIPE1 and AQP1 in renal cortical tissue from patients with DN and patients with minor lesions.(n = 4.Bar = 50 μm). **D**: Representative images and statistical graphs of colocalization of TIPE1 and AQP1 in kidney tissues from WT and STZ-induced DN mice by immunofluorescence staining. (n = 4.Bar = 50 μm). **E-F**: Western blot analysis (E) and densitometric quantification (F) of TIPE1 and KIM-1 expression in kidney cortical tissues from WT mice (n = 6) and DN mice (n = 5). **G**: RT-qPCR analysis of TIPE1 and KIM1 expression in kidney tissues. **H–I**: Western blot analysis (H) and densitometric quantification (I) of TIPE1 and KIM1 in HK-2 cells treated with high glucose. **J**: RT-qPCR analysis of TIPE1 in HK-2 cells. Results are expressed as the mean ± SEM. *P < 0.05; **P < 0.01; ***P < 0.001.

captured with an Olympus optical microscope.

2.8. Seahorse analysis

The mitochondrial oxygen consumption rate (OCR) was assessed using the mitochondrial stress test kit (Agilent,103015100). In brief, 10,000 cells per well were seeded and allowed to stand for 1 h to allow cells to settle naturally. Cells were placed in a 37 °C CO_2 cell culture chamber overnight. Next, 200 μL of XF calibration fluid were added to the wells for the hydration probe plate in the culture chamber without CO_2 for 45–60 min. We prepared 100 ml detection liquid containing 1 ml glucose, 1 mL pyruvate, and 1 mL glutamine. Cells were washed twice with detection liquid twice, 160 μl detection liquid were added per well. The plate was cultured in a 37 °C cell culture chamber without CO_2 for 1 h before testing. Oligomycin (2 μM), FCCP (2-[2-[4-(trifluoromethoxy) phenyl] hydrazinylidene]-propanedinitrile) (2 μM), and rotenone (0.5 μM) combined with antimycin (0.5 μM) were injected sequentially. The OCR was normalized to the cell number per well.

2.9. ATP detection

ATP production was estimated using an ATP detection kit (Beyotime S0026). In brief, 200 μl lysate were added to 20 mg of kidney tissue and homogenized with a glass homogenizer. Lysates were centrifuged at 12000 g at 4 °C for 5 min. Then, the lysates were incubated with 100 μl of ATP detection solution in 96-well plates and tested using the luciferase assay.

2.10. Histological analysis

Kidney tissues were fixed in 4% paraformaldehyde for 24 h and embedded in paraffin. Paraffin sections (4 μm) were deparaffinized and rehydration. Kidney sections were stained with standard hematoxylin and eosin (HE). Histopathological kidney injury was also evaluated.

2.11. Immunofluorescence and immunohistochemical staining

For immunofluorescence staining, cells were fixed, blocked with 30% goat serum, and incubated with primary antibodies (Table S2). After washing with PBS, the cells were incubated with fluorescence-conjugated secondary antibodies (Table S2), and nuclei were counterstained with DAPI. Images were detected with an Olympus optical microscope or captured by confocal laser-scanning microscopy and analyzed using Zen2010 software.

For immunohistochemical staining, 2 μM thick paraffin-embedded kidney sections were subjected to routine staining. Kidney sections were incubated with primary antibodies for 2 h at room temperature and incubated with secondary antibodies for 30 min at 37 °C. Nuclei were counterstained with hematoxylin. Image analysis and quantification were performed using Image J.

2.12. Protein half-life assay

Control or TIPE1 knockdown HK-2 cells were treated with 500 μg/mL cycloheximide (S7418, Selleck) for 0, 2, 4, and 6 h, respectively. Cell lysates were collected to analyze the protein levels of PHB2 by western blotting. Quantification of PHB2 protein expression was normalized to that of β-actin at different time points using Image J software.

2.13. In vivo ubiquitination assay

HEK293 cells were co-transfected with HA-tagged ubiquitin, pcTIPE1, or pcDNA3. Forty-eight hours later, the cells were treated with MG132 for 6 h. The cell lysates were immunoprecipitated with anti-PHB2 antibody and then subjected to western blotting with antibodies specific against Ub and HA.

2.14. Western blot analysis

Total proteins were extracted by incubating the cell pellet or kidney in RIPA buffer (P0013D, Beyotime) supplemented with 1% PMSF and 1% phosphatase inhibitors. Protein concentration was measured using a BCA protein quantitative kit (P0011, Beyotime). For the extraction of mitochondrial proteins, the mitochondria were first isolated from the cell pellet or kidney tissues after incubation with mitochondrial separation reagent (C3606, C3601, Beyotime), followed by grinding with a glass homogenizer. Isolated mitochondria were resuspended in RIPA buffer for protein extraction.

Proteins were separated by sodium dodecyl sulfate-polyacrylamide gel electrophoresis (SDS-PAGE) and transferred to a polyvinylidene fluoride (PVDF) membrane. After blocking with 5% albumin bovine V (Solarbio A8020) at room temperature for 1 h, the membrane was incubated with the primary antibodies (Table S2) at 4 °C overnight. After washing with TBST, the membrane was incubated with horseradish peroxidase (HRP)-labeled secondary antibodies at room temperature for 1 h, and exposed to ECL reagent (WBKLS0500, Millipore).

2.15. RNA extraction and real-time PCR analysis

Total RNA was extracted from renal cortical tissue or cultured cells using TRIzol (15596-018, Invitrogen, Carlsbad, CA, USA) and reverse transcribed into cDNA. Real-time PCR was performed using SYBR Green reagent on a Bio-Rad CFX PCR System (Bio-Rad, Carlsbad, CA, USA).

2.16. Detection of apoptosis by flow cytometry and TUNEL staining

DNA fragmentation was detected in situ using a TUNEL staining kit according to the manufacturer's instructions (C1090, Beyotime). Images were analyzed using a fluorescence microscope (DP80, Olympus). TUNEL-positive nuclei were counted using the ImageJ software (version 1.8.0).

Apoptosis of cultured cells was estimated by flow cytometry. Cells were treated with normal and high glucose for 48 h and stained with APC-Annexin V and 7AAD at room temperature for 15 min, and subsequently analyzed using a flow cytometer (CytoFLEX S, Beckman, USA).

2.17. Statistical analysis

Data are expressed as the mean ± SEM. Student's *t*-test was employed for comparisons between two groups, and one-way analysis of variance (ANOVA) followed by Tukey's post-test for multiple comparisons was used for groups of three or more. Statistical significance was set

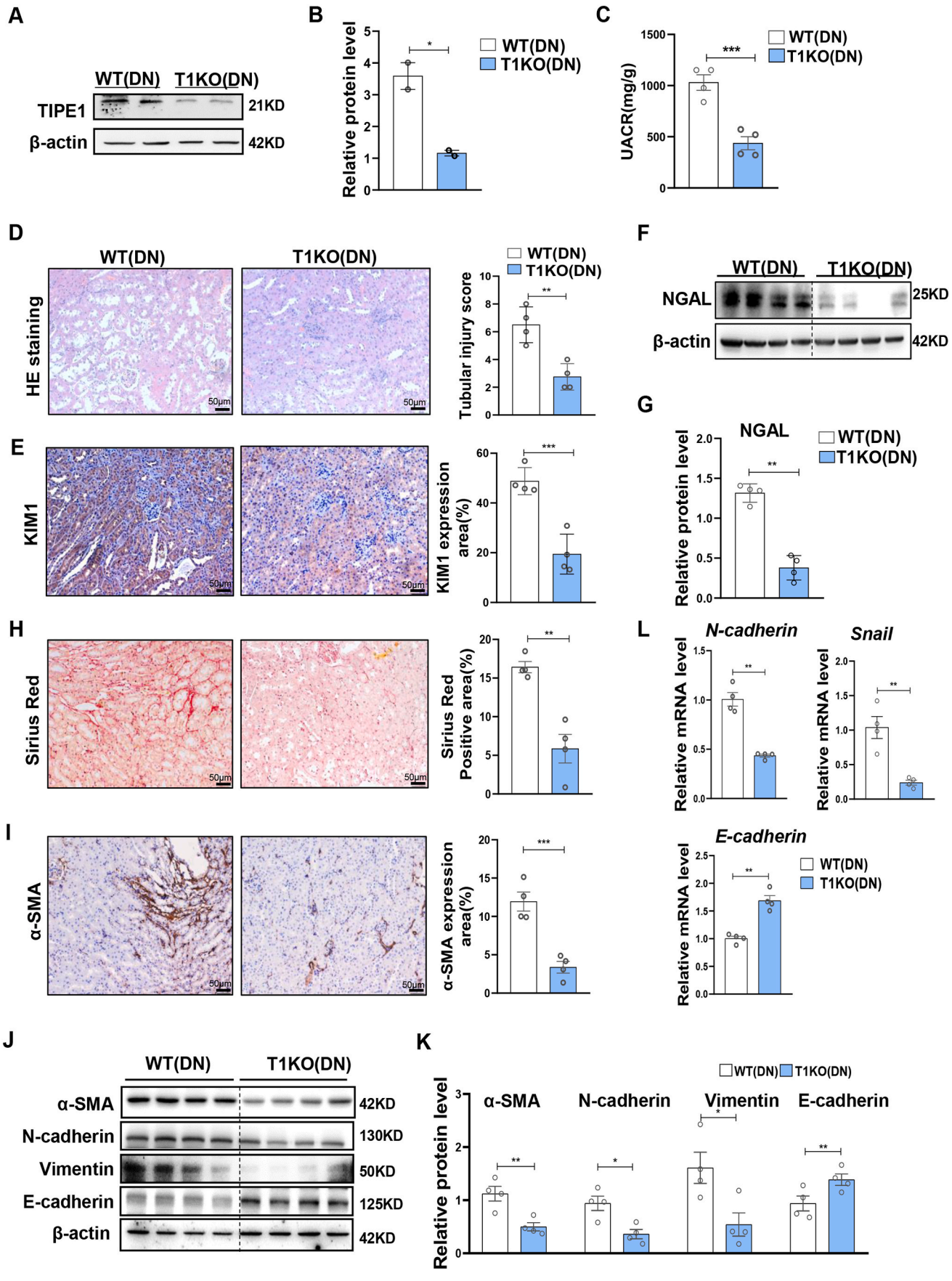

(caption on next page)

Fig. 2. Deficiency of *Tipe1* in RTECs alleviates diabetic renal injury and fibrosis.
A-B: Western blot analysis (A) and densitometric quantification (B) of TIPE1 expression in kidney tissues from WT and T1KO mice. **C–K**: TIKO and WT mice were subjected to STZ-induced DN, and kidney function and damage were evaluated. (n = 4).**C**: Urinary ACRs. **D**: Representative images and statistical graphs of H&E staining of the kidney. (n = 4).**E**: Representative images and statistical graphs of immunohistochemical staining of KIM1 in kidney sections. (n = 4).**F-G**: Western blot analysis (F) and densitometric quantification (G) of NAGL expression in kidney tissues. (n = 4). **H**: Representative images and statistical graphs of Sirius red staining of kidney tissues. **I**: Immunohistochemical staining for α-SMA in the kidneys. (n = 4).**J-L**: Western blot (J,K) and RT-qPCR (L) analysis for the expression of α-SMA,N-cadherin, Vimentin and E-cadherin in kidney tissues. (n = 4). Results were expressed as means ± SEMs. *P < 0.05; **P < 0.01; ***P < 0.001.

at $p < 0.05$. In vitro and *in vivo* experiments were performed in at least three independent experiments. Differences were evaluated using GraphPad Prism. Statistical significance was set at $p < 0.05$. *P < 0.05, **P < 0.01, ***P < 0.001.

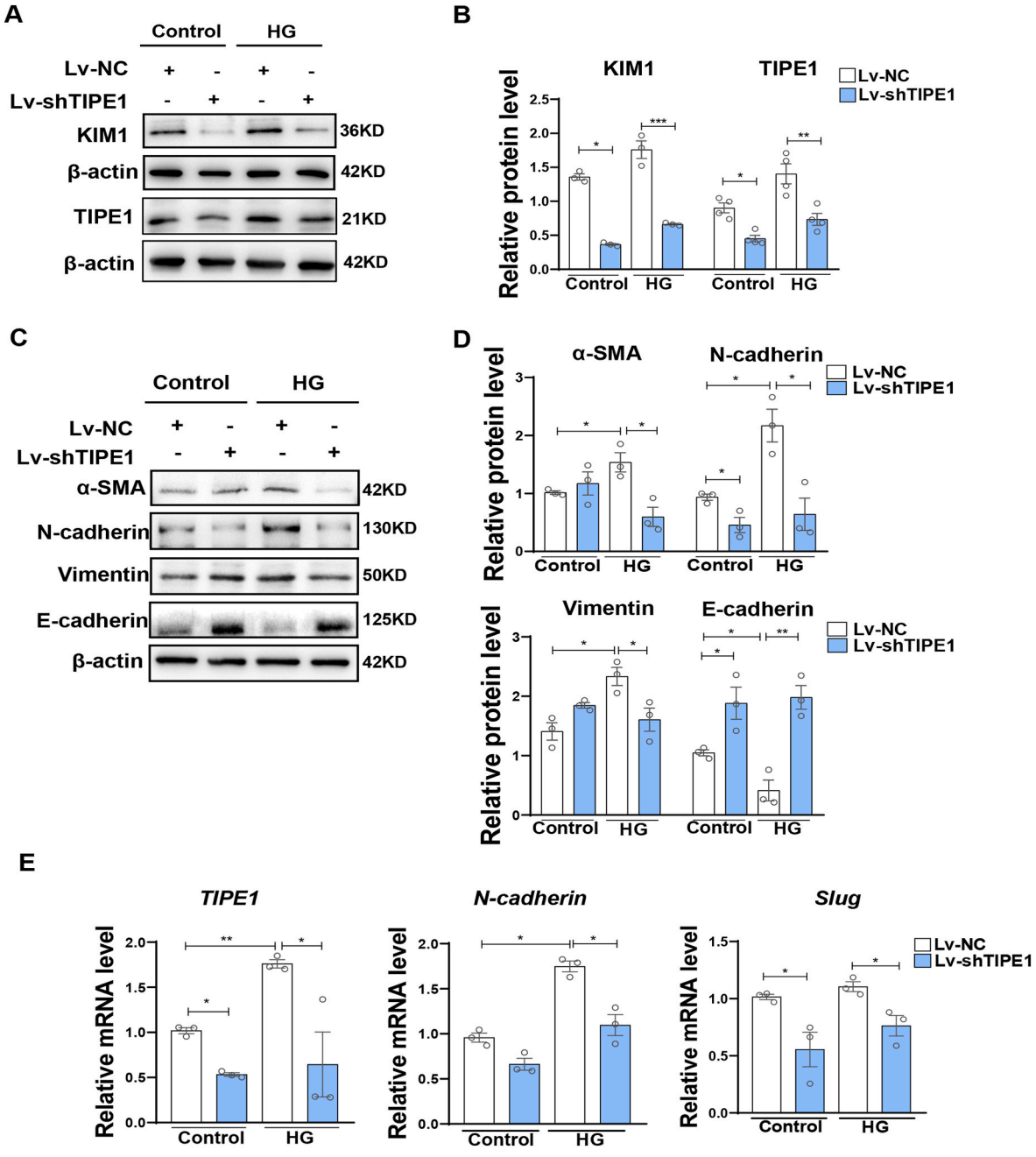

Fig. 3. TIPE1 knockdown ameliorates HK-2 cell injury and EMT under HG ambience.
HK-2 cells were infected with Lv-NC or Lv-TIPE1 and screened using puromycin (1 μg/ml). The cells were then treated with 40 mM glucose for 48 h. **A-B**: Western blot analysis (A) and densitometric quantification (B) of KIM1 and TIPE1 expression. **C-D**: Western blot analysis (C) and densitometric quantification (D) of α-SMA, N-cadherin, vimentin, and E-cadherin. **E**: RT-qPCR analysis of *TIPE1, N-cadherin*, and *Slug*. Results were expressed as means ± SEMs. *P < 0.05; **P < 0.01; ***P < 0.001.

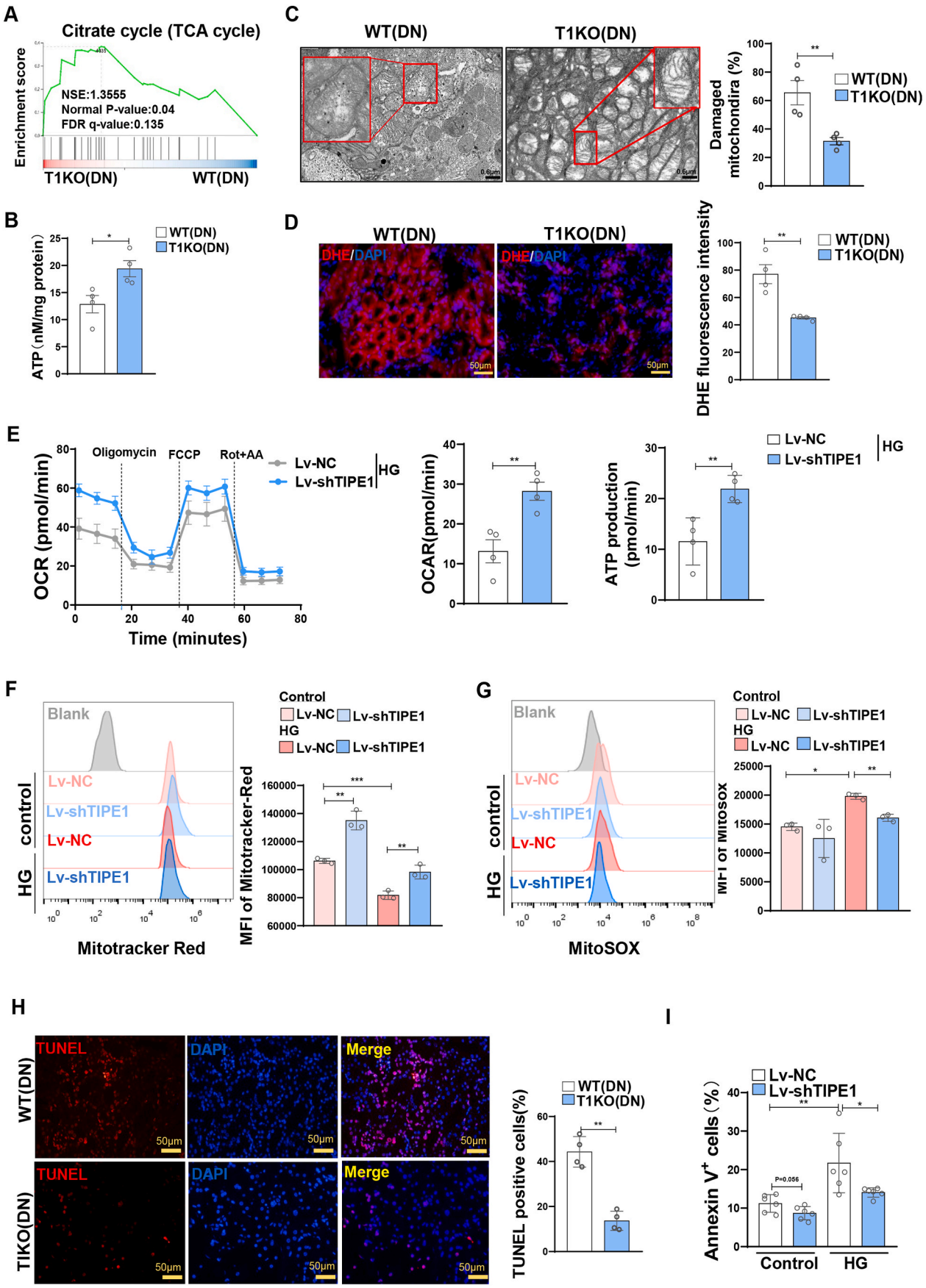

(caption on next page)

Fig. 4. *Tipe1* deficiency improves mitochondrial homeostasis and decreases apoptosis of RTECs under HG ambience.
A-D: Kidney tissues from WT and T1KO mice with STZ-induced DN.(n = 4). **A**: Renal tissues from WT and T1KO mice were subjected to RNA sequencing. GSEA analysis of the citrate cycle for differentially expressed genes (DEGs). **B**: ATP levels in WT and T1KO mice with STZ-induced DN. **C**: TEM images of mitochondrial morphology and statistical graphs of damaged mitochondria. (Bar=0.6 μm). **D**: Representative images and statistical graphs of DHE staining. (Bar = 0.6 μm) **E**. Representative OCR analysis and statistical graph of HG-treated HK-2 cells, upon addition of oligomycin (Oligo), the mitochondrial decoupler FCCP, and rotenone (Rot) + antimycin (AA). **F-G**: Representative plots and statistical graphs for flow cytometry analysis of MitoTracker-red (F) and MitoSox (G) in HK-2 cells infected with Lv-NC or Lv-TIPE1 and treated with 40 mM glucose for 48 h. **H**: Representative images and statistical graphs of TUNEL staining of kidney tissues from WT and T1KO mice with STZ-induced DN. **I**: Statistical graphs of flow cytometry analysis for Annexin V/7-AAD staining of control or HG-treated HK-2 cells infected with Lv-NC or Lv-TIPE1. Results were expressed as means ± SEMs. *P < 0.05; **P < 0.01; ***P < 0.001.

3. Results

3.1. TIPE1 expression is up-regulated in RTECs of DN patients and mice

To preliminarily assess the potential involvement of TIPE1 in DN, we first analyzed the expression of TIPE1 in DN patients and healthy donors (HD) using data from the Nephroseq Database. The result showed that TIPE1 expression was significantly increased in the DN group compared to that in the healthy donor group (Fig. 1A). Immunohistochemical staining further confirmed the upregulation of TIPE1 in renal tissues of DN patients (Fig. 1B), as well as in STZ-induced diabetic mice (Supplementary Figs. 1A–E). Strikingly, immunofluorescence staining revealed that upregulated TIPE1 expression was mainly observed in proximal tubular cells (marked by AQP1) in both DN patients and mice (Fig. 1C and D), whereas TIPE1 staining in glomeruli remained unaffected (Supplementary Fig. 1F). Western blot and RT-qPCR analysis further validated the upregulation of TIPE1 in the renal tissues of DN mice, which coincided with the elevated level of KIM1, a marker for kidney tubular injury (Fig. 1E–G). In accordance with this, TIPE1 expression was also upregulated in HK-2 cells with different concentrations of glucose (20 mM and 40 mM) and for different time points (24 h and 48 h), accompanied by increased expression of KIM1, N-cadherin, and α-SMA (Fig. 1H–J, Supplementary Figs. 2A–D). Together, these results demonstrated that TIPE1 expression was increased in RTECs of diabetic kidney tissues, indicating the potential involvement of TIPE1 in the pathogenesis of DN.

3.2. Tipe1 deficiency in RTECs alleviates renal injury and fibrosis in DN

To further evaluate the role of TIPE1 in tubular cells in DN progression, we generated proximal tubular cell-specific *Tipe1* knockout mice (T1KO) by crossing Ksp-cre and *Tipe1*$^{f/f}$ mice, thus confirming TIPE1 knockout efficiency (Fig. 2A and B). Importantly, *Tipe1* deficiency decreased the urine protein creatinine ratio (UACR) (Fig. 2C) and significantly mitigated STZ-induced renal tubular injury, as indicated by HE staining (Fig. 2D) and the expression of the tubular damage markers, KIM1 and NGAL (Fig. 2E–G, Supplementary Fig. 3). The excessive deposition of extracellular matrix (ECM) proteins in the renal tubulointerstitium is a key event in the progression of DN [8,10]. Thus, we further evaluated the degree of interstitial fibrosis and EMT of tubular cells. Ablation of *Tipe1* in RTECs led to reduced collagen accumulation, as indicated by Sirius red staining and α-SMA expression (Fig. 2H and I). Accordingly, the expression of mesenchymal cell markers (vimentin and N-cadherin) and TFs (Snail) was significantly downregulated, while the level of epithelial cell markers (E-cadherin) was increased in *Tipe1* deficient mice after STZ treatment (Fig. 2J-L). These results indicate that *Tipe1* deficiency in RTECs rescued tubular cell damage and alleviated renal EMT and fibrosis in DN.

We further confirmed the involvement of TIPE1 in HG-induced tubular damage using human renal tubular epithelial cells HK-2. Consistent with our *in vivo* data, compared to the negative control shRNA lentivirus (Lv-NC), lentivirus carrying *Tipe1* shRNA (Lv-sh*TIPE1*) significantly reduced the expression of KIM1 in HK-2 cells under HG treatment (Fig. 3A and B). Accordingly, *Tipe1* silencing also downregulated the expression of mesenchymal cell markers and TFs, but upregulated the expression of epithelial markers in HK-2 cells, especially under HG conditions (Fig. 3C–E). Together, these results strongly support the view that TIPE1 expression promotes tubular cell damage, EMT, and renal fibrosis, thereby accelerating DN progression.

3.3. Ablation of Tipe1 improves mitochondrial homeostasis and decreases apoptosis of RTECs under HG ambience

To further investigate how TIPE1 modulates HG-induced damage and EMT progression in RTECs, we performed transcriptomic analysis of the renal cortex of WT and TIKO mice with STZ-induced DN. RNA-sequencing (RNA-seq) revealed a total of 1166 differentially expressed genes (DEGs), defined by a fold change ≥2.00, adjusted p value ≤ 0.001 (Supplementary Fig. 4A). Gene Set Enrichment Analysis (GSEA) revealed the enrichment of gene sets related to the AGE-RAGE signaling pathway in diabetic complications, ECM-receptor interaction, and proximal tubule bicarbonate reclamation in the renal cortex tissues of T1KO mice relative to those of WT mice (Supplementary Figs. 4B–D), confirming the regulation of tubular cell TIPE1 and its role in renal damage and EMT process.

Interestingly, genes related to the tricarboxylic acid (TCA) cycle were positively enriched in the renal cortex tissues of T1KO mice compared to those of WT mice (Fig. 4A). Consistently, ATP levels in the kidney tissues of T1KO mice were higher than those in WT mice (Fig. 4B). Transmission electron microscopy (TEM) revealed that RTECs from STZ-induced T1KO mice had a significantly decreased ratio of damaged mitochondria, as indicated by mitochondrial swelling, fracture of the inner and/or outer membranes, and rupture of the mitochondrial crest (Fig. 4C). Moreover, DHE staining revealed decreased levels of ROS in the renal tissues of T1KO mice (Fig. 4D). In accordance with the *in vivo* data, oxygen consumption rate (OCR) analysis showed that silencing of *Tipe1* in HK-2 cells elevated the oxidative phosphorylation capacity and ATP production (Fig. 4E). Furthermore, *Tipe1* knockdown upregulated mitochondrial membrane potential, but downregulated mitochondrial ROS levels in HG-treated HK-2 cells, as indicated by MitoTracker Red and MitoSOX staining, respectively (Fig. 4F and G). Consistent with the determinant roles of mitochondria in controlling cell viability [28], deficiency of *Tipe1* in RTECs significantly reduced the ratio of TUNEL-positive nuclei in the renal tissues (Fig. 4H). Decreased apoptosis was also observed in Lv-shTIPE1 infected HK-2 cells under HG conditions (Fig. 4I, Supplementary Fig. 4F). Altogether, these results demonstrate that TIPE1 has the ability to modulate mitochondrial homeostasis and cell viability in tubular cells, which in turn determine the progression of DN.

3.4. Enhanced mitophagy by Tipe1 deletion protects RTECs from HG-induced damage and EMT

Next, we investigated how TIPE1 controls mitochondrial homeostasis in RTECs. Mitophagy is a process of eliminating damaged mitochondria to maintain homeostasis. KEGG pathway analysis of the RNAseq data revealed that mitophagy-related genes were significantly enriched in renal tissues from T1KO mice relative to that in WT mice (Fig. 5A); of these, genes related to mitophagy induction, including *Pink1*, *Parkin*, *Atg12*, *and Mfn1/2,* were upregulated, whereas *Sqstm1/p62* and *Rps27a* genes were downregulated in the renal tissues of T1KO mice (Fig. 5B). Western blot analysis confirmed the upregulated protein

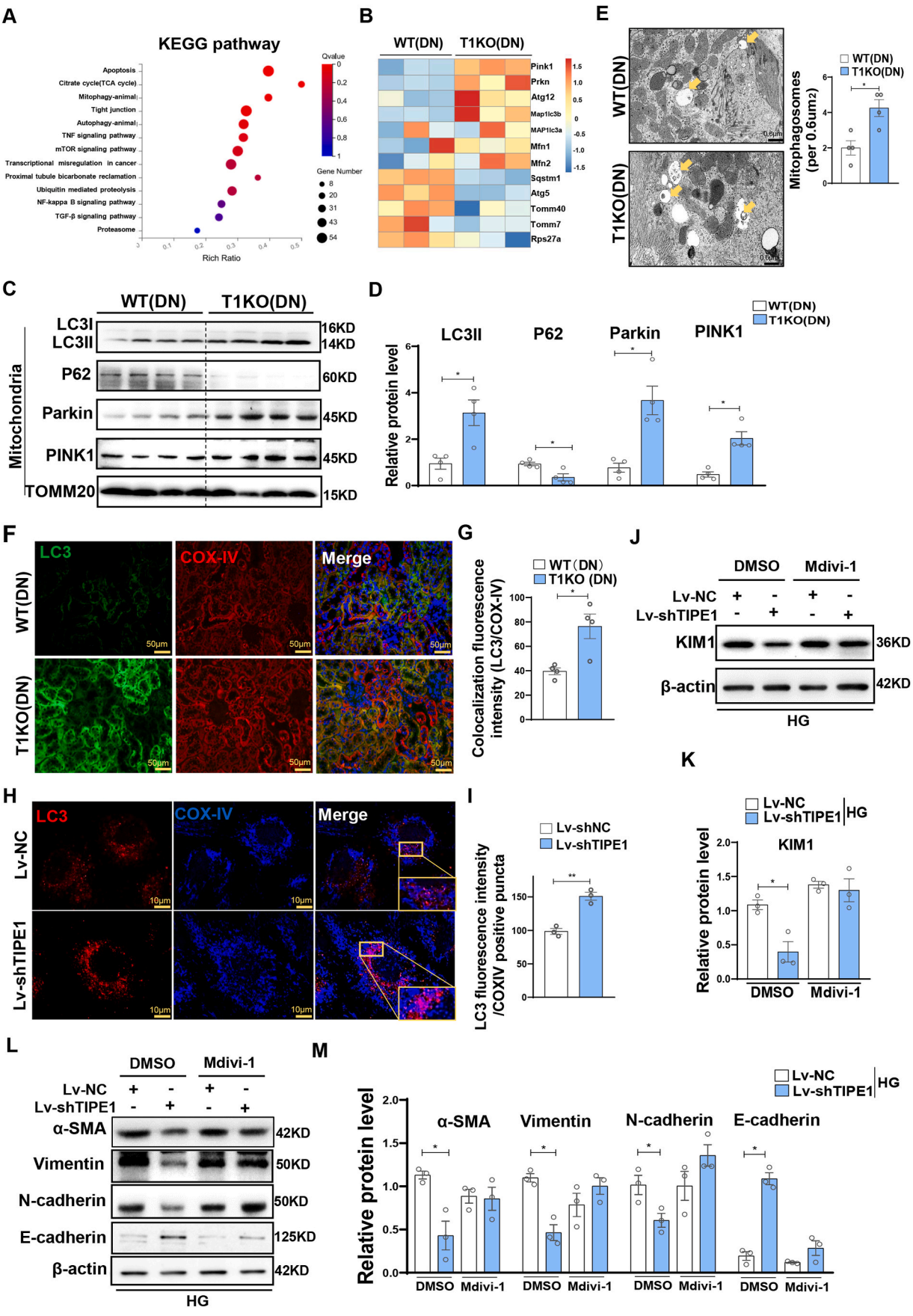

(caption on next page)

Fig. 5. Enhanced mitophagy by *Tipe1* ablation alleviates HG-induced damage and EMT of RTECs.
A-B: RNAseq data analysis of kidney tissues from WT and T1KO mice with STZ-induced DN. **A**: KEGG pathway analysis of the DEGs. **B**: Heatmap analysis of the expression of mitophagy-related genes. **C-D**: Western blot analysis (C) and densitometric quantification (D) of LC3I/II, P62, Parkin, and PINK1 expression in mitochondrial fractions from kidney tissues of WT and T1KO mice. **E**: Representative TEM images and statistical graphs of mitophagosomes in kidney tissues from WT and T1KO mice. (Bar = 0.6 μm). **F-G:** Representative images and statistical graphs for immunofluorescence staining of LC3 and COX-IV in kidney tissues of WT and T1KO mice. (Bar = 50 μm). **H–I**: Representative TEM images and statistical graphs for immunofluorescence staining of LC3 and COX-IV in Lv-NC or Lv-shTIPE1 infected HK-2 cells.(Bar = 10 μm) **J-M:** Western blot analysis and densitometric quantification of KIM1 (J-K) and α-SMA, vimentin, N-cadherin, and E-cadherin expression (L-M) in Lv-NC or Lv-shTIPE1-infected HK-2 cells treated with 40 mM glucose and/or Mdivi-1(5 μM) for 6 h. Results were expressed as means ± SEMs. *P < 0.05; **P < 0.01.

levels of PINK1, Parkin, and LC3II, and the reduced expression of p62 in the mitochondrial fraction of renal tissues from T1KO mice compared to those in WT mice (Fig. 5C and D). Consistently, TEM revealed there were more mitochondrial autophagosomes in the renal tissues from T1KO mice than those in WT mice with STZ-induced DN (Fig. 5E). Co-localization of LC3 with COX-IV, an indicative marker of mitophagy, was more prominent in the renal tissues of T1KO mice compared to that in WT mice (Fig. 5F and G). Similar results were also found in Lv-shTIPE1 infected HK-2 cells under HG conditions (Fig. 5H and I, Supplementary Fig. 5A). These results demonstrate that TIPE1 is a potential mitophagy inhibitor in RTECs.

Accumulating data demonstrated mitophagy as the important mechanism underlying selective degradation of defective mitochondria, involved in kidney injury and repair [29]. To further validate the importance of dysregulated mitophagy in TIPE1 promotion on tubular cell damage under HG ambience, we pretreated HK-2 cells with the mitophagy inhibitor Mdivi-1 [30,31], and observed that the upregulation of PINK1 expression in Lv-shTIPE1 infected HK-2 cells was almost abrogated (Supplementary Figs. 5B–C). More importantly, treatment with Mdivi-1 attenuated the downregulated expression of KIM1 in HK-2 cells by knockdown of TIPE1 (Fig. 5J and K). Consistently, Mdivi-1 treatment significantly rescued the enhanced EMT promotion of TIPE1 silencing in HK-2 cells, displaying comparable levels of EMT markers (α-SMA, vimentin, N-cadherin, and E-cadherin) in Mdivi-1 treated control or *Tipe1* knockdown HK-2 cells (Fig. 5L-M). Taken together, these data strongly suggest that ablation of *Tipe1* enhanced mitophagy in RTECs, which in turn slow down tubular cell damage and EMT.

3.5. TIPE1 interacts with and promotes the proteasomal degradation of PHB2

Next, we investigated the mechanisms by which TIPE1 modulates the mitophagy of RTECs. Accumulating evidence has shown that TIPE1 interacts with various proteins to regulate cellular biology [32]. Thus, we performed LC-MS/MS using immunoprecipitants from pcTIPE1-HA transfected cells (Fig. 6A). There were 30 potential interacting proteins with protein scores greater than 200 (Supplementary Table 3). Among them (Fig. 6B), prohibitin 2 (PHB2) has been reported to be an inner mitochondrial membrane protein and functions as a crucial mitophagy receptor in both mammalian cells and *C. elegans* [33]. Co-immunoprecipitation assays demonstrated the interaction of TIPE1 and PHB2 in pcTIPE1-HA transfected HEK293 cells (Fig. 6C). The endogenous association was further validated in control or HG-treated HK-2 cells (Fig. 6D). Furthermore, PHB2 protein, mainly in mitochondria, was upregulated in Lv-shTIPE1 infected HK-2 cells under HG conditions, while *PHB2* mRNA was comparable with Lv-NCinfected cells (Fig. 6E–G, Supplementary Figs. 6A–B). Immunofluorescence staining confirmed this effect (Supplementary Fig. 6C). Cycloheximide (CHX) chase assay further revealed that TIPE1 knockdown increased the half-life of the PHB2 protein in HK-2 cells (Fig. 6H and I). Moreover, treatment with the proteasome inhibitor (MG132), but not the autophagy inhibitor chloroquine (CQ), abrogated the upregulation of PHB2 induced by TIPE1 silencing in HK-2 cells (Fig. 6J and K), indicating that TIPE1 promotes proteasomal degradation of PHB2. Consistently, ectopic TIPE1 expression led to increased ubiquitination of PHB2 in HEK293 cells (Fig. 6L). Together, these results indicate that TIPE1 interacts with PHB2 and accelerates its degradation by the ubiquitin-proteasome pathway.

3.6. Knockdown of PHB2 abrogates the improvement of Tipe1 deficiency in mitophagy, damage and EMT of RTECs

Next, we investigated whether PHB2 dysregulation is responsible for TIPE1 promotion in HG-induced tubular cell damage and DN progression. HG treatment downregulated the expression and mitochondrial localization of PHB2 in HK2 cells (Supplementary Figs. 7A–B). These results indicate that PHB2 dysregulation may be involved in the pathogenesis of DN. To verify its involvement in the regulation of TIPE1 in mitophagy and damage in RTECs, WT or T1KO mice were injected with lentiviruses encoding *PHB2* shRNA (Lv-sh*PHB2*) or negative control lentivirus (Lv-NC). We found that PHB2 knockdown almost abolished the effect of Tipe1 deficiency on mitophagy in RTECs, as indicated by the comparable levels of Parkin, PINK1, LC3II/I, and PHB2 in the mitochondria of renal tissues from WT and T1KO mice (Fig. 7A and B). Moreover, there were no significant differences in mitophagy, mitochondrial membrane potential, or ROS levels between PHB2 shRNA-transfected control and TIPE1 knockdown HK-2 cells (Supplementary Figs. 8A–D). Consistently, silencing of PHB2 also abrogated the expression difference of NGAL (Fig. 7C and D), as well as that of EMT markers (α-SMA, N-cadherin, and E-cadherin), between the renal tissues from WT and T1KO mice (Fig. 7E and F). HE and immunohistochemical staining further confirmed that PHB2 knockdown almost abolished the additional improvement of tubular cell *Tipe1* deficiency on renal damage and fibrosis (Fig. 7G). Similar effects were also observed for the EMT tendency of HK-2 cells under HG conditions (Supplementary Figs. 8E–F). Together, these results strongly support the view that tubular cell TIPE1 suppresses mitophagy and promotes DN progression by dysregulating the expression of PHB2.

3.7. Tubular cell TIPE1 correlates with renal function, mitophagy and fibrosis in DN patients

To explore the clinical implications of TIPE1 in human DN, we further analyzed the correlation between TIPE1 expression and renal function. Data from the Nephroseq Database revealed that TIPE1 expression was negatively correlated with the glomerular filtration rate (GFR) (ml/min·1.73 m^2) in DN patients (Fig. 8A). We then examined the expression of TIPE1, PHB2, and α-SMA in kidney biopsies from DN patients (Fig. 8B). Statistical analysis showed that there was a negative correlation between TIPE1 expression and UACR in DN patients (Fig. 8C). Moreover, TIPE1 levels were positively associated with α-SMA expression, but negatively associated with PHB2 expression (Fig. 8D and E). These results further support the view that TIPE1 functions as a promoting factor in DN progression.

4. Discussion

This study establishes the crucial role of TIPE1 in RTECs in the regulation of DN progression. Our results demonstrate that TIPE1 impairs PINK1/Parkin-mediated mitophagy and disrupts mitochondrial homeostasis in RTECs under HG conditions. It is clear from our data that TIPE1 upregulation is a catalyst of RTEC damage and EMT, which

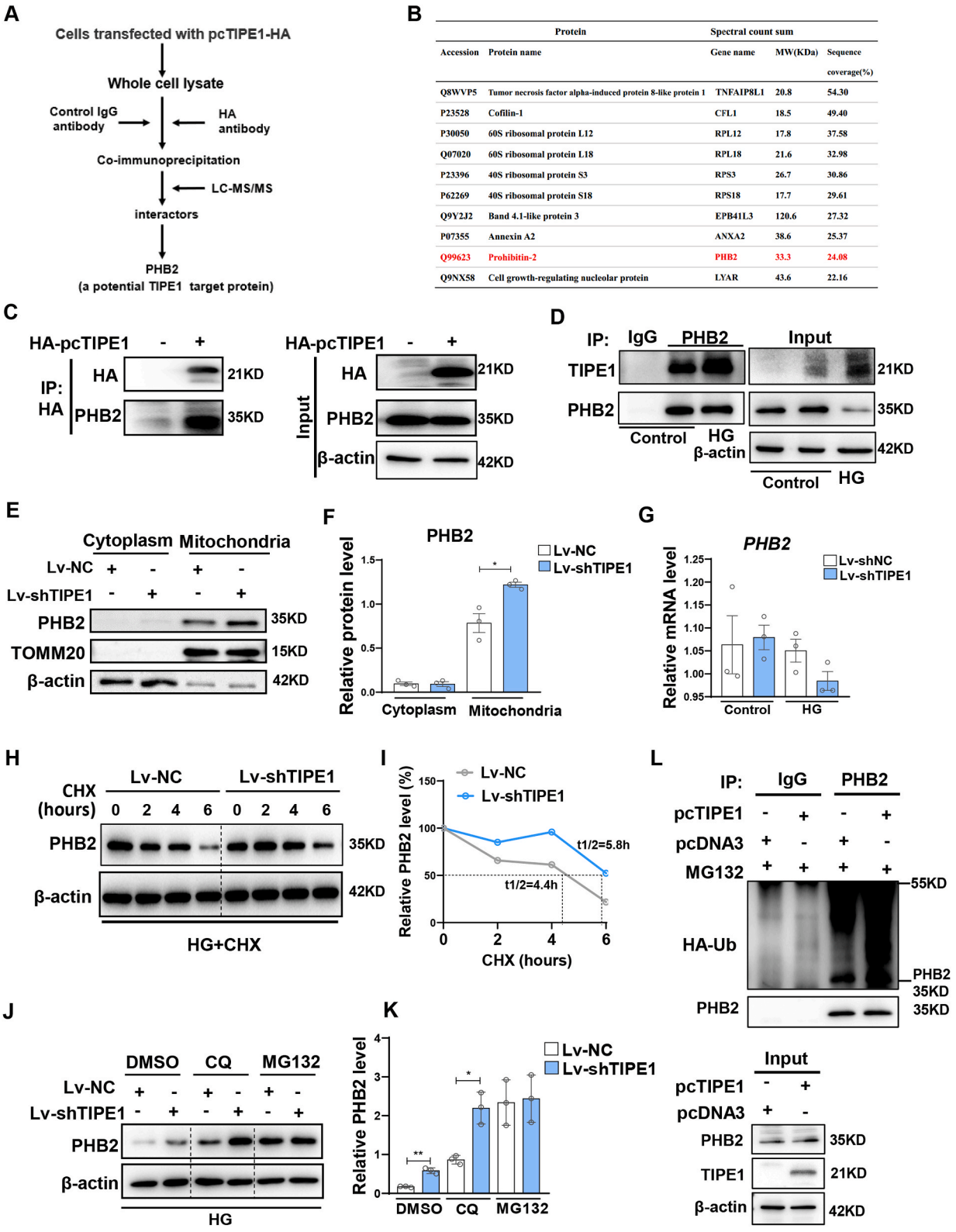

Protein		Spectral count sum		
Accession	Protein name	Gene name	MW(KDa)	Sequence coverage(%)
Q8WVP5	Tumor necrosis factor alpha-induced protein 8-like protein 1	TNFAIP8L1	20.8	54.30
P23528	Cofilin-1	CFL1	18.5	49.40
P30050	60S ribosomal protein L12	RPL12	17.8	37.58
Q07020	60S ribosomal protein L18	RPL18	21.6	32.98
P23396	40S ribosomal protein S3	RPS3	26.7	30.86
P62269	40S ribosomal protein S18	RPS18	17.7	29.61
Q9Y2J2	Band 4.1-like protein 3	EPB41L3	120.6	27.32
P07355	Annexin A2	ANXA2	38.6	25.37
Q99623	Prohibitin-2	PHB2	33.3	24.08
Q9NX58	Cell growth-regulating nucleolar protein	LYAR	43.6	22.16

Fig. 6. TIPE1 interacts with and promotes the proteasomal degradation of PHB2.
A-B: Proteomic mass spectrometry analysis of Huh7 cells transfected with empty vector or HA-TIPE1 plasmids for 48 h. **A**: Schematic diagram. **B**: Top 10 candidate interacting proteins. **C**: Co-immunoprecipitation assay for the interaction of PHB2 with TIPE1 in HEK-293 cells transfected with the empty vector or HA-TIPE1 plasmids for 48 h. **D**: Co-immunoprecipitation analysis investigating interaction of endogenous TIPE1 with PHB2 in HK-2 cells with or without HG treatment. **E-F**: Western blotting analysis (E) and densitometric quantification (F) of PHB2 expression in the mitochondrial and cytosolic fractions of HK-2 cells. **G:** RT-qPCR analysis of PHB2 expression in Lv-NC or Lv-shTIPE1 infected HK-2 cells. **H–I:** Cycloheximide (CHX) chase assay for PHB2 in Lv-NC or Lv-shTIPE1 infected HK-2 cells treated with CHX (500 μg/ml) for the indicated time points. **J-K**: Western blot analysis (J) and densitometric quantification (K) of PHB2 in Lv-NC or Lv-shTIPE1 infected HK-2 cells treated with 10 μM CQ or 10 μM MG132 for 6 h under HG conditions. **L**: Co-immunoprecipitation assay for the ubiquitination of PHB2 in HEK293 cells transfected with pcTIPE1 and ubiquitin-expressing plasmids and treated with MG132. Results were expressed as means ± SEMs. *P < 0.05; **P < 0.01.

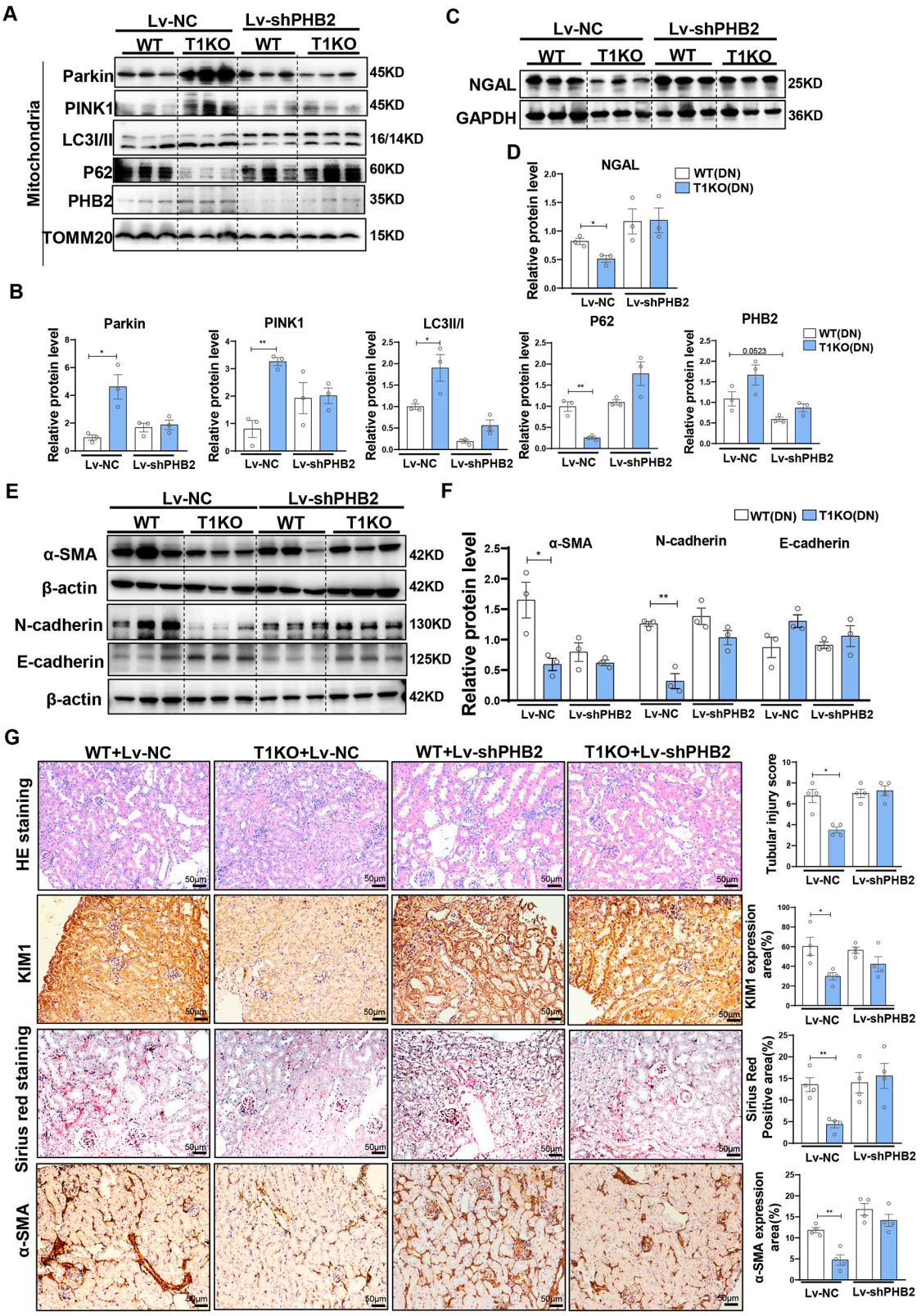

Fig. 7. Knockdown of PHB2 abrogates the improvement of *Tipe1* deficiency on mitophagy, damage and EMT of RTECs.
WT or T1KO mice were intrarenally injected with lentiviruses encoding PHB2 shRNA (Lv-shPHB2) or negative control lentiviruses (Lv-NC) and subjected to STZ-induced DN (n = 4). Renal cortical tissues were used for further analyses. **A-B**: Western blot analysis (A) and densitometric quantification (B) of LC3I/II, P62, PINK1, Parkin, and PHB2 expression in the mitochondrial fraction. **C–F**: Western blot analysis (**C, E**) and densitometric quantification (**D, F**) of NGAL, α-SMA, N-cadherin, and E-cadherin. **G**: Representative images and statistical graphs for HE staining, KIM1 immunohistochemical staining, Sirius red staining, and α-SMA immunohistochemical staining. (Bar = 50 μm). Results were expressed as means ± SEMs. *P < 0.05; **P < 0.01.

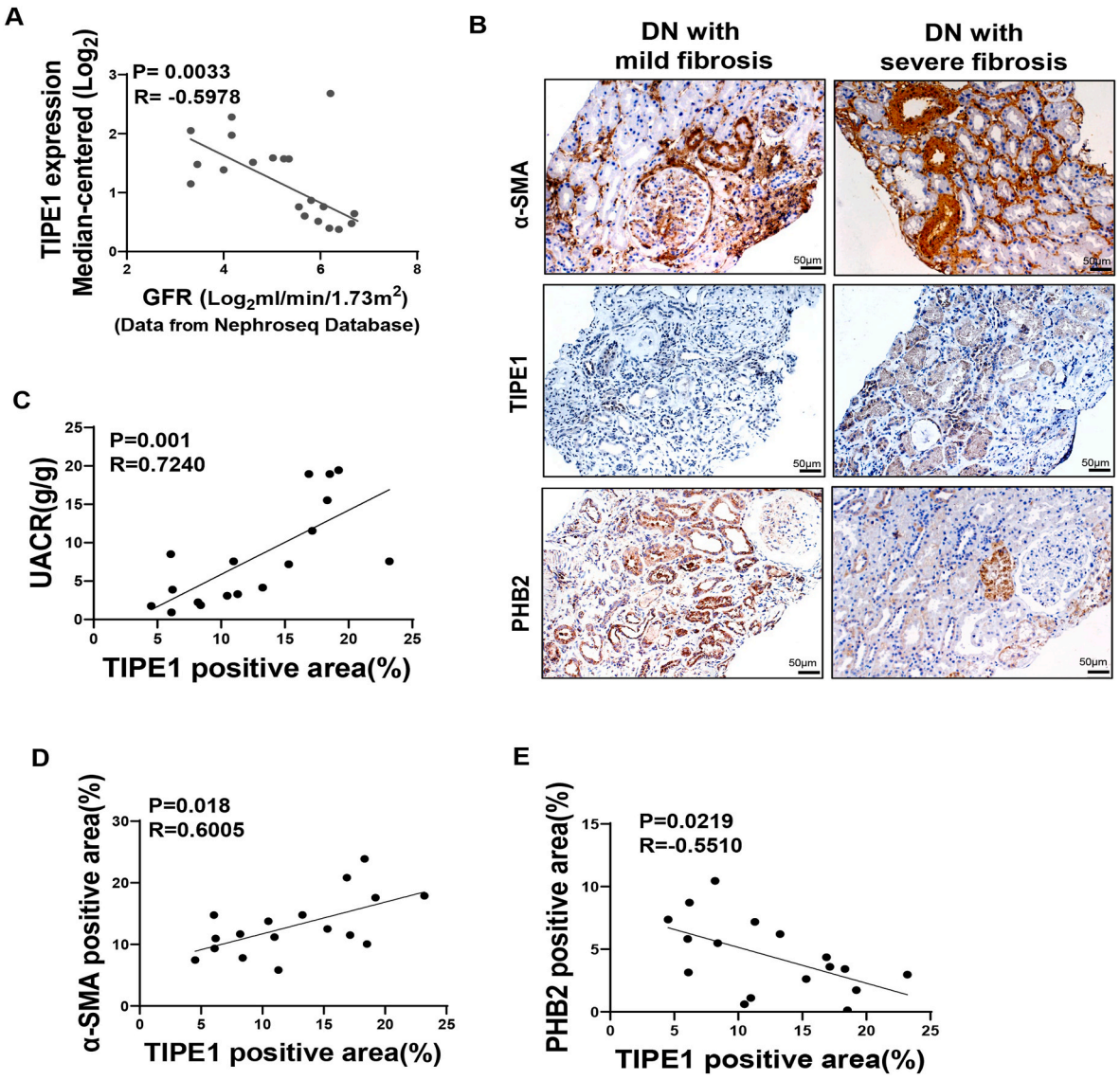

Fig. 8. TIPE1 expression in RTECs correlates with renal function, mitophagy and fibrosis in DN patients. A: Correlation analysis of TIPE1 and GFR with DN patient data from the Nephroseq Database (P = 0.0033, R = −0.5978). **B**. Representative images for immunohistochemical staining of TIPE1, α-SMA and PHB2 expression in needle renal biopsy specimens from subjects with DN (n = 17). (Bar = 100 μm). **C**: Correlation analysis of UACR with the intensity of TIPE1(P = 0.001, R = 0.7240). **D-E**: Correlation of TIPE1 intensity with α-SMA (D)(P = 0.018, R = 0.6005) and PHB2 (E)(P = 0.0219, R = −0.5510).

ultimately promote the development of DN (Fig. 9).

RTEC is the main component of the renal parenchyma, and in recent years the importance of tubular injury has been emphasized in the pathogenesis of diabetic kidney diseases [34]. Tubular damage has been reported to be a better and independent predictor for the progression of DN [35]. Furthermore, these approaches targeting the tubular compartment were verified to benefit the overall amelioration of DN [13,36,37]. TIPE1 is ubiquitously expressed in various tissues, but seems to be unevenly distributed across different cell types in an indicated tissue. Our data demonstrated that TIPE1 expression was predominantly present in the RTECs of human and mouse renal tissues, and was significantly upregulated in DN patients and mice models, in a manner distinct from the increase in TIPE and TIPE2 expression mainly observed in diabetic glomeruli [20]. Importantly, TIPE1 intensity in RTECs was correlated with the severity of tubulointerstitial fibrosis and the decline of renal function. Consistently, RTEC-specific loss of *Tipe1* not only dramatically attenuated tubular cell death and EMT, but also improved renal function (i.e., decreased urinary ACR) in STZ-induced diabetic mice. Although the mechanisms by which high glucose upregulates the expression of TIPE1 remain to be investigated, these results identify TIPE1 as a crucial regulator of tubular cell damage in diabetic kidney diseases.

RTECs are enriched in mitochondria to meet high metabolic energy demands, and as such, they are vulnerable to the disorder of mitochondrial bioenergetics [26,37]. In fact, insufficient ATP production in tubular mitochondria is associated with various kidney diseases, including DN [15,38,39]. Accumulating evidence indicates that defects in mitochondrial dynamics and excessive mitochondrial oxidative stress are the primary causative factors of tubular injury in DN [37]. Therefore, a number of novel mitochondria-targeted strategies are currently in development for the treatment of kidney diseases [40,41]. In this study, we found that ablation of *Tipe1* in RTECs significantly improved mitochondrial morphology and membrane potential, while decreasing mitochondrial ROS levels under HG conditions. Accordingly, *Tipe1* deficiency reduced the apoptosis rate of tubular cells. These data suggest that TIPE1 contributes to HG-induced tubular cell death by disrupting mitochondrial homeostasis. TIPE1 was first identified as a candidate molecule for involvement in both necroptosis and apoptosis [21]. Later,

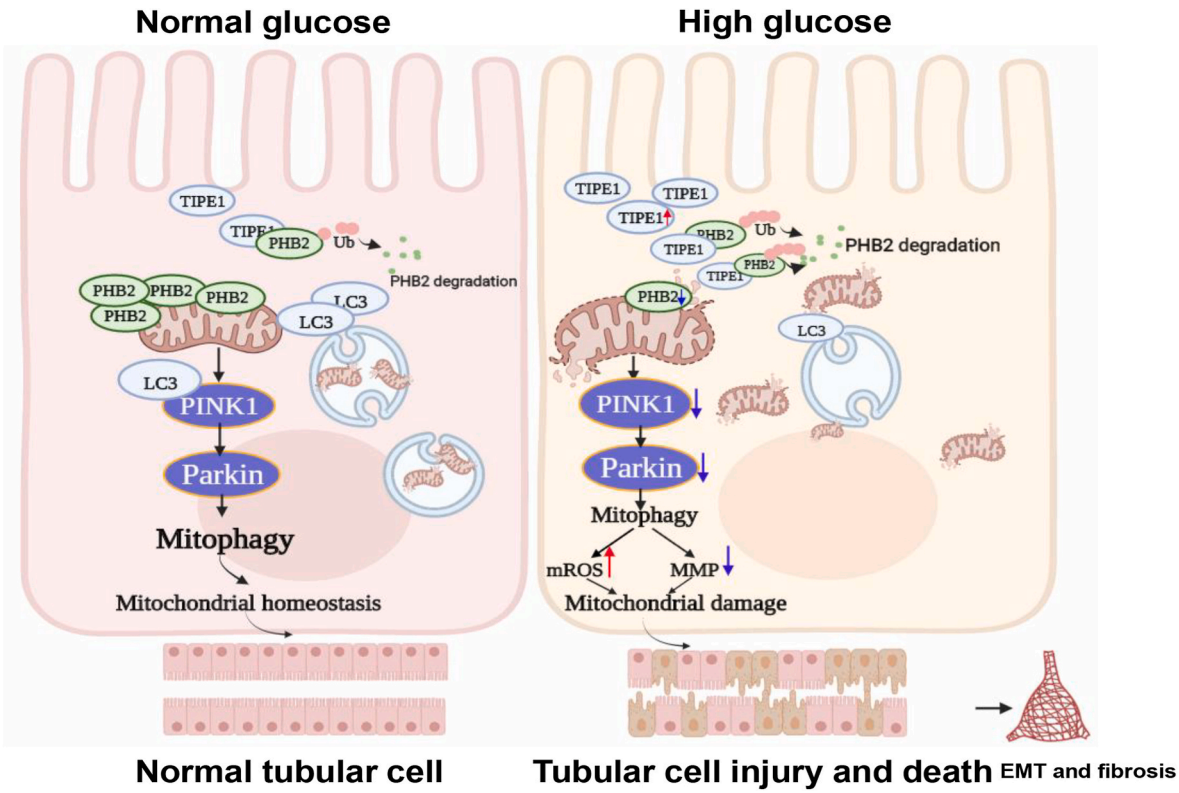

Fig. 9. TIPE1 upregulation in RTECs aggravates DN progression via disrupting PHB2 mediated mitophagy. The upregulation of TIPE1 in RTECs under HG ambience interacts with PHB2 and triggers its proteasomal degradation, which in turn disrupts mitophagy and mitochondrial homeostasis, and promotes the progression of DN.

TIPE1 was reported to modulate cell death by acting on multiple signaling pathways, such as the Rac1 [22] and p53 [42] pathways. To the best of our knowledge, this is the first report to demonstrate that TIPE1 disrupts mitochondrial homeostasis and leads to cell death, highlighting the versatile regulatory mechanisms of TIPE1 in manipulating cell fate.

The most intriguing finding of the present study is that TIPE1 suppresses mitophagy of RTECs by interacting with PHB2 and promoting its proteasomal degradation, which in turn aggravates DN progression. Mitophagy is an important mitochondrial quality control mechanism that selectively eliminates damaged mitochondria [43]. Defects in mitophagy are associated with various pathological conditions, including DN [44]. However, the mechanisms of dysregulated mitophagy in DN are somewhat limited. Here, we found that deficiency of *Tipe1* enhanced the mitophagy of RTECs, thus illustrating the mechanism by which TIPE1 regulates mitochondrial homeostasis. Mechanistically, PHB2 knockdown almost abolished the promotion of *Tipe1* ablation on tubular cell mitophagy and improved diabetic kidney function. PHB2 was recently reported to be a crucial regulator of Parkin-induced mitophagy as either a mitophagy receptor to bind with LC3 or a mitochondrial stabilizer for PINK1 in mammalian cells [30,45]. Mitophagy inhibition with PHB2 knockdown was similar to that induced by knockdown of ATG727, and *Phb2* null mice have been found to be early embryonic lethal [46], indicating the importance of PHB2 in mitophagy induction and tissue maintenance. However, the regulatory mechanisms underlying PHB2-mediated mitophagy remain largely unknown. It was first reported that Bax inhibitor-1 (BI1) interacts with cytoplasmic PHB2 and facilitates its mitochondrial import, which is essential for maintaining renal tubular function [47]. In the present study, we first demonstrated that the stabilization of PHB2 in RTECs was disrupted by TIPE1 overexpression through ubiquitin-proteasomal mediated degradation. Interestingly, TIPE1 was previously reported to competitively bind to FBXW5, a subunit of the SCF-type E3 ubiquitin ligase complex, and to prevent the degradation of tuberous sclerosis complex 2 (TSC2) [48]. Although the E3 ligase involved in TIPE1-mediated PHB2 degradation remains to be further investigated, these observations should help to uncover a novel regulatory mechanism for PHB2-mediated mitophagy.

In summary, our results demonstrated that the upregulation of TIPE1 contributes to HG-induced RTEC damage and DN progression by impairing PHB2-mediated mitophagy. These findings should shed new light on therapeutic strategies for diabetic kidney diseases.

Disclosure of interest

All the authors declared no competing interests.

Author contributions

LL performed the research, interpreted the data, and wrote the manuscript. LL, FB, HS, XLR and SJL performed the research. RX, YZW and HMY provided material and skills and assisted in establishing techniques. XHL CHM, LFG and XDY designed the experiment, critically reviewed and approved the manuscript.

Acknowledgement

This study was supported by grants from the National Natural Science Foundation of China (No. 81970508, 82070746), the National Key Research and Development Program (2018YFE0126500), the National Natural Science Fund for Outstanding Youth Fund (82000692). We thank Translational Medicine Core Facility of Shandong University for consultation and instrument availability that supported this work.

Appendix A. Supplementary data

Supplementary data to this article can be found online at https://doi.org/10.1016/j.redox.2022.102260.

References

[1] K. Umanath, J.B. Lewis, Update on diabetic nephropathy: Core curriculum 2018, Am. J. Kidney Dis. 71 (6) (2018) 884–895.
[2] Q. Han, H. Zhu, X. Chen, Z. Liu, Non-genetic mechanisms of diabetic nephropathy, Front. Med. 11 (3) (2017) 319–332.
[3] A.M. Warren, S.T. Knudsen, M.E. Cooper, Diabetic nephropathy: an insight into molecular mechanisms and emerging therapies, Expert Opin. Ther. Targets 23 (7) (2019) 579–591.
[4] B.L. Neuen, T. Young, H.J.L. Heerspink, SGLT2 inhibitors for the prevention of kidney failure in patients with type 2 diabetes: a systematic review and meta-analysis, Lancet Diabetes Endocrinol. 7 (11) (2019) 845–854.
[5] N. Perico, P. Ruggenenti, G. Remuzzi, ACE and SGLT2 inhibitors: the future for non-diabetic and diabetic proteinuric renal disease, Curr. Opin. Pharmacol. 33 (2017) 34–40.
[6] R.S. Gaston, G. Basadonna, F.G. Cosio, et al., Transplantation in the diabetic patient with advanced chronic kidney disease: a task force report, Am. J. Kidney Dis. 44 (3) (2004) 529–542.
[7] S.C.W. Tang, W.H. Yiu, Innate immunity in diabetic kidney disease, Nat. Rev. Nephrol. 16 (4) (2020) 206–222.
[8] V. Vallon, S.C. Thomson, The tubular hypothesis of nephron filtration and diabetic kidney disease, Nat. Rev. Nephrol. 16 (6) (2020) 317–336.
[9] M. Ruiz-Ortega, S. Rayego-Mateos, S. Lamas, A. Ortiz, R.R. Rodrigues-Diez, Targeting the progression of chronic kidney disease, Nat. Rev. Nephrol. 16 (5) (2020) 269–288.
[10] Y. Liu, Cellular and molecular mechanisms of renal fibrosis, Nat. Rev. Nephrol. 7 (12) (2011) 684–696.
[11] H. Muraoka, K. Hasegawa, Y. Sakamaki, et al., Role of Nampt-Sirt6 Axis in renal proximal tubules in extracellular matrix deposition in diabetic nephropathy, Cell Rep. 27 (1) (2019) 199–212, e5.
[12] M.L. Brezniceanu, C.J. Lau, N. Godin, et al., Reactive oxygen species promote caspase-12 expression and tubular apoptosis in diabetic nephropathy, J. Am. Soc. Nephrol. 21 (6) (2010) 943–954.
[13] R.E. Gilbert, Proximal tubulopathy: Prime mover and key therapeutic target in diabetic kidney disease, Diabetes 66 (4) (2017) 791–800.
[14] Z. Tian, M. Liang, Renal metabolism and hypertension, Nat. Commun. 12 (1) (2021) 963.
[15] T. Micakovic, S. Papagiannarou, E. Clark, et al., The angiotensin II type 2 receptors protect renal tubule mitochondria in early stages of diabetes mellitus, Kidney Int. 94 (5) (2018) 937–950.
[16] L. Sun, P. Xie, J. Wada, et al., Rap1b GTPase ameliorates glucose-induced mitochondrial dysfunction, J. Am. Soc. Nephrol. 19 (12) (2008) 2293–2301.
[17] W. Wang, Y. Wang, J. Long, et al., Mitochondrial fission triggered by hyperglycemia is mediated by ROCK1 activation in podocytes and endothelial cells, Cell Metabol. 15 (2) (2012) 186–200.
[18] K. Sharma, B. Karl, A.V. Mathew, et al., Metabolomics reveals signature of mitochondrial dysfunction in diabetic kidney disease, J. Am. Soc. Nephrol. 24 (11) (2013) 1901–1912.
[19] G. Padmavathi, K. Banik, J. Monisha, et al., Novel tumor necrosis factor-α induced protein eight (TNFAIP8/TIPE) family: functions and downstream targets involved in cancer progression, Cancer Lett. 432 (2018) 260–271.
[20] S. Zhang, Y. Zhang, X. Wei, et al., Expression and regulation of a novel identified TNFAIP8 family is associated with diabetic nephropathy, Biochim. Biophys. Acta 1802 (11) (2010) 1078–1086.
[21] J. Hitomi, D.E. Christofferson, A. Ng, et al., Identification of a molecular signaling network that regulates a cellular necrotic cell death pathway, Cell 135 (7) (2008) 1311–1323.
[22] Z. Zhang, X. Liang, L. Gao, et al., TIPE1 induces apoptosis by negatively regulating Rac1 activation in hepatocellular carcinoma cells, Oncogene 34 (20) (2015) 2566–2574.
[23] Y. Liu, X. Qi, Z. Zhao, et al., TIPE1-mediated autophagy suppression promotes nasopharyngeal carcinoma cell proliferation via the AMPK/mTOR signaling pathway, J. Cell Mol. Med. 24 (16) (2020) 9135–9144.
[24] D. Bordoloi, G. Padmavathi, K. Banik, et al., Human tumor necrosis factor alpha-induced protein eight-like 1 exhibited potent anti-tumor effect through modulation of proliferation, survival, migration and invasion of lung cancer cells, Mol. Cell. Biochem. 476 (9) (2021) 3303–3318.
[25] J. Cui, G. Zhang, C. Hao, et al., The expression of TIPE1 in murine tissues and human cell lines, Mol. Immunol. 48 (12–13) (2011) 1548–1555.
[26] L. Xiao, X. Xu, F. Zhang, The mitochondria-targeted antioxidant MitoQ ameliorated tubular injury mediated by mitophagy in diabetic kidney disease via Nrf2/PINK1, Redox Biol. 11 (2017) 297–311.
[27] M. Liu, K. Liang, J. Zhen, et al., Sirt6 deficiency exacerbates podocyte injury and proteinuria through targeting Notch signaling, Nat. Commun. 8 (1) (2017) 413.
[28] F.J. Bock, S.W.G. Tait, Mitochondria as multifaceted regulators of cell death, Nat. Rev. Mol. Cell Biol. 21 (2) (2020) 85–100.
[29] C. Tang, J. Cai, X.M. Yin, J.M. Weinberg, M.A. Venkatachalam, Z. Dong, Mitochondrial quality control in kidney injury and repair, Nat. Rev. Nephrol. 17 (5) (2021) 299–318.
[30] K. Mizumura, S.M. Cloonan, K. Nakahira, et al., Mitophagy-dependent necroptosis contributes to the pathogenesis of COPD, J. Clin. Invest. 124 (9) (2014) 3987–4003.
[31] X. Zhang, H. Yan, Y. Yuan, et al., Cerebral ischemia-reperfusion-induced autophagy protects against neuronal injury by mitochondrial clearance [published correction appears in Autophagy, Autophagy 9 (9) (2013) 1321–1333, 2019 Jun;15(6):1124].
[32] J.R. Goldsmith, S. Fayngerts, Y.H. Chen, Regulation of inflammation and tumorigenesis by the TIPE family of phospholipid transfer proteins, Cell. Mol. Immunol. 14 (6) (2017) 482–487.
[33] Y. Wei, W.C. Chiang, R. Sumpter Jr., P. Mishra, B. Levine, Prohibitin 2 is an inner mitochondrial membrane mitophagy receptor, Cell 168 (1–2) (2017) 224–238, e10.
[34] C. Jia, C. Ke-Hong, X. Fei, et al., Decoy receptor 2 mediation of the senescent phenotype of tubular cells by interacting with peroxiredoxin 1 presents a novel mechanism of renal fibrosis in diabetic nephropathy, Kidney Int. 98 (3) (2020) 645–662.
[35] S.C. Tang, K.N. Lai, The pathogenic role of the renal proximal tubular cell in diabetic nephropathy, Nephrol. Dial. Transplant. 27 (8) (2012) 3049–3056.
[36] M. Zhan, I.M. Usman, L. Sun, Y.S. Kanwar, Disruption of renal tubular mitochondrial quality control by Myo-inositol oxygenase in diabetic kidney disease, J. Am. Soc. Nephrol. 26 (6) (2015) 1304–1321.
[37] G.C. Higgins, M.T. Coughlan, Mitochondrial dysfunction and mitophagy: the beginning and end to diabetic nephropathy? Br. J. Pharmacol. 171 (8) (2014) 1917–1942.
[38] H.Y. Lin, Y. Chen, Y.H. Chen, et al., Tubular mitochondrial AKT1 is activated during ischemia reperfusion injury and has a critical role in predisposition to chronic kidney disease, Kidney Int. 99 (4) (2021) 870–884.
[39] S.M. Tan, M. Ziemann, V. Thallas-Bonke, et al., Complement C5a induces renal injury in diabetic kidney disease by disrupting mitochondrial metabolic agility, Diabetes 69 (1) (2020) 83–98.
[40] H.H. Szeto, Pharmacologic approaches to improve mitochondrial function in AKI and CKD, J. Am. Soc. Nephrol. 28 (10) (2017) 2856–2865.
[41] W. Dai, H. Lu, Y. Chen, D. Yang, L. Sun, L. He, The loss of mitochondrial quality control in diabetic kidney disease, Front. Cell Dev. Biol. 9 (2021) 706832.
[42] P. Zhao, X. Pang, J. Jiang, et al., TIPE1 promotes cervical cancer progression by repression of p53 acetylation and is associated with poor cervical cancer outcome, Carcinogenesis 40 (4) (2019) 592–599.
[43] M. Onishi, K. Yamano, M. Sato, N. Matsuda, K. Okamoto, Molecular mechanisms and physiological functions of mitophagy, EMBO J. 40 (3) (2021), e104705.
[44] S.A. Killackey, D.J. Philpott, S.E. Girardin, Mitophagy pathways in health and disease, J. Cell Biol. 219 (11) (2020), e202004029.
[45] C. Yan, L. Gong, L. Chen, et al., PHB2 (prohibitin 2) promotes PINK1-PRKN/Parkin-dependent mitophagy by the PARL-PGAM5-PINK1 axis, Autophagy 16 (3) (2020) 419–434.
[46] C. Merkwirth, S. Dargazanli, T. Tatsuta, et al., Prohibitins control cell proliferation and apoptosis by regulating OPA1-dependent cristae morphogenesis in mitochondria, Genes Dev. 22 (4) (2008) 476–488.
[47] J. Wang, P. Zhu, R. Li, J. Ren, Y. Zhang, H. Zhou, Bax inhibitor 1 preserves mitochondrial homeostasis in acute kidney injury through promoting mitochondrial retention of PHB2, Theranostics 10 (1) (2020) 384–397.
[48] J.Y. Ha, J.S. Kim, Y.H. Kang, E. Bok, Y.S. Kim, J.H. Son, Tnfaip8 l1/Oxi-β binds to FBXW5, increasing autophagy through activation of TSC2 in a Parkinson's disease model, J. Neurochem. 129 (3) (2014) 527–538.